NATIONAL ADVISORY COMMITTEE FOR AERONAUTICS

REPORT No. 569

WING-NACELLE-PROPELLER INTERFERENCE FOR WINGS OF VARIOUS SPANS FORCE AND PRESSURE-DISTRIBUTION TESTS

By RUSSELL G. ROBINSON and WILLIAM H. HERRNSTEIN, Jr.

1936

AERONAUTIC SYMBOLS

1. FUNDAMENTAL AND DERIVED UNITS

	Symbol	Metric		English	
		Unit	Abbreviation	Unit	Abbreviation
Length	l	meter	m	foot (or mile)	ft. (or mi.)
Time	t	second	s	second (or hour)	sec. (or hr.)
Force	F	weight of 1 kilogram	kg	weight of 1 pound	lb.
Power	P	horsepower (metric)		horsepower	hp.
Speed	V	{kilometers per hour	k.p.h.	miles per hour	m.p.h.
		{meters per second	m.p.s.	feet per second	f.p.s.

2. GENERAL SYMBOLS

W, Weight $= mg$

g, Standard acceleration of gravity $= 9.80665$ m/s² or 32.1740 ft./sec.²

m, Mass $= \dfrac{W}{g}$

I, Moment of inertia $= mk^2$. (Indicate axis of radius of gyration k by proper subscript.)

μ, Coefficient of viscosity

ν, Kinematic viscosity

ρ, Density (mass per unit volume)

Standard density of dry air, 0.12497 kg-m⁻⁴-s² at 15° C. and 760 mm; or 0.002378 lb.-ft.⁻⁴-sec.²

Specific weight of "standard" air, 1.2255 kg/m³ or 0.07651 lb./cu.ft.

3. AERODYNAMIC SYMBOLS

S, Area

S_w, Area of wing

G, Gap

b, Span

c, Chord

$\dfrac{b^2}{S}$, Aspect ratio

V, True air speed

q, Dynamic pressure $= \dfrac{1}{2}\rho V^2$

L, Lift, absolute coefficient $C_L = \dfrac{L}{qS}$

D, Drag, absolute coefficient $C_D = \dfrac{D}{qS}$

D_o, Profile drag, absolute coefficient $C_{D_o} = \dfrac{D_o}{qS}$

D_i, Induced drag, absolute coefficient $C_{D_i} = \dfrac{D_i}{qS}$

D_p, Parasite drag, absolute coefficient $C_{D_p} = \dfrac{D_p}{qS}$

C, Cross-wind force, absolute coefficient $C_C = \dfrac{C}{qS}$

R, Resultant force

i_w, Angle of setting of wings (relative to thrust line)

i_t, Angle of stabilizer setting (relative to thrust line)

Q, Resultant moment

Ω, Resultant angular velocity

$\rho\dfrac{Vl}{\mu}$, Reynolds Number, where l is a linear dimension (e.g., for a model airfoil 3 in. chord, 100 m.p.h. normal pressure at 15° C., the corresponding number is 234,000; or for a model of 10 cm chord, 40 m.p.s. the corresponding number is 274,000)

C_p, Center-of-pressure coefficient (ratio of distance of c.p. from leading edge to chord length)

α, Angle of attack

ϵ, Angle of downwash

α_o, Angle of attack, infinite aspect ratio

α_i, Angle of attack, induced

α_a, Angle of attack, absolute (measured from zero-lift position)

γ, Flight-path angle

REPORT No. 569

WING-NACELLE-PROPELLER INTERFERENCE FOR WINGS OF VARIOUS SPANS FORCE AND PRESSURE-DISTRIBUTION TESTS

By RUSSELL G. ROBINSON and WILLIAM H. HERRNSTEIN, JR.

Langley Memorial Aeronautical Laboratory

NATIONAL ADVISORY COMMITTEE FOR AERONAUTICS

HEADQUARTERS, NAVY BUILDING, WASHINGTON, D. C.

LABORATORIES, LANGLEY FIELD, VA.

Created by act of Congress approved March 3, 1915, for the supervision and direction of the scientific study of the problems of flight (U. S. Code, Title 50, Sec. 151). Its membership was increased to 15 by act approved March 2, 1929. The members are appointed by the President, and serve as such without compensation.

JOSEPH S. AMES, Ph. D., *Chairman*,
    Baltimore, Md.

DAVID W. TAYLOR, D. Eng., *Vice Chairman*,
    Washington, D. C.

CHARLES G. ABBOT, Sc. D.,
    Secretary, Smithsonian Institution.

LYMAN J. BRIGGS, Ph. D.,
    Director, National Bureau of Standards.

ARTHUR B. COOK, Rear Admiral, United States Navy,
    Chief, Bureau of Aeronautics, Navy Department.

WILLIS RAY GREGG, B. A.,
    Chief, United States Weather Bureau.

HARRY F. GUGGENHEIM, M. A.,
    Port Washington, Long Island, N. Y.

SYDNEY M. KRAUS, Captain, United States Navy,
    Bureau of Aeronautics, Navy Department.

CHARLES A. LINDBERGH, LL. D.,
    New York City.

WILLIAM P. MACCRACKEN, Jr., LL. D.,
    Washington, D. C.

AUGUSTINE W. ROBINS, Brigadier General, United States Army,
    Chief Matériel Division, Air Corps, Wright Field, Dayton, Ohio.

EUGENE L. VIDAL, C. E.,
    Director of Air Commerce, Department of Commerce.

EDWARD P. WARNER, M. S.,
    New York City.

OSCAR WESTOVER, Major General, United States Army,
    Chief of Air Corps, War Department.

ORVILLE WRIGHT, Sc. D.,
    Dayton, Ohio.

GEORGE W. LEWIS, *Director of Aeronautical Research*

JOHN F. VICTORY, *Secretary*

HENRY J. E. REID, *Engineer in Charge, Langley Memorial Aeronautical Laboratory, Langley Field, Va.*

JOHN J. IDE, *Technical Assistant in Europe, Paris, France*

TECHNICAL COMMITTEES

AERODYNAMICS
POWER PLANTS FOR AIRCRAFT
AIRCRAFT STRUCTURES AND MATERIALS

AIRCRAFT ACCIDENTS
INVENTIONS AND DESIGNS

Coordination of Research Needs of Military and Civil Aviation

Preparation of Research Programs

Allocation of Problems

Prevention of Duplication

Consideration of Inventions

LANGLEY MEMORIAL AERONAUTICAL LABORATORY

LANGLEY FIELD, VA.

Unified conduct, for all agencies, of scientific research on the fundamental problems of flight.

OFFICE OF AERONAUTICAL INTELLIGENCE

WASHINGTON, D. C.

Collection classification, compilation, and dissemination of scientific and technical information on aeronautics.

REPORT No. 569

WING-NACELLE-PROPELLER INTERFERENCE FOR WINGS OF VARIOUS SPANS FORCE AND PRESSURE-DISTRIBUTION TESTS

By Russell G. Robinson and William H. Herrnstein, Jr.

SUMMARY

An experimental investigation was made in the N. A. C. A. full-scale wind tunnel to determine the effect of wing span on nacelle-propeller characteristics and, reciprocally, the lateral extent of nacelle and propeller influence on a monoplane wing. The results provide a check on the validity of the previous research on nacelles and propellers with 15-foot-span wings tested in the 20-foot wind tunnel and reported in Technical Reports 415, 436, 462, 505, 506, and 507.

The 4/9-scale propeller and the N. A. C. A. cowling used in the former researches were tested in three typical tractor locations with respect to a thick wing of 5-foot chord and 30-foot span. The span was progressively reduced to 25, 20, and 15 feet and the same characteristics were measured in each case.

The efficiency factors—propulsive efficiency, nacelle drag efficiency, and net efficiency—were obtained for each wing length by means of force tests and the values are compared to determine the effect of span. Pressure-distribution measurements show the lateral extent of the nacelle interference and the propeller-slipstream effect on the span loading for the various conditions. Complete polar curves and curves showing the variation of nacelle drag with lift coefficient are also included.

Force and pressure-distribution tests concur in indicating that, for engineering purposes, the influence of a nacelle and of a propeller, in a usual combination, may be considered to extend laterally on a wing the same maximum distance, or about five nacelle diameters or two propeller diameters outboard of their common axes. All important effects of 4/9-scale nacelle-propeller combinations may be measured within practical limits of accuracy by tests of a 15-foot-span wing.

INTRODUCTION

Several years of research in the N. A. C. A. 20-foot tunnel have provided data comparing the merits of most practicable wing-nacelle-propeller combinations for air-cooled radial engines. There have been tested a tractor propeller with an N. A. C. A. cowled nacelle and a thick wing (reference 1), with various radial-engine cowlings and a thick wing (reference 2), with various radial-engine cowlings and a Clark Y wing (reference 3); tandem propellers with a thick wing and various radial-engine cowlings (reference 4); a tractor propeller with a Clark Y biplane cellule and N. A. C. A. cowled nacelle (reference 5); and a pusher propeller with various wings and radial-engine cowlings (reference 6). For all these investigations a 4/9-scale reproduction of a Wright J-5 Whirlwind engine was used in conjunction with engine nacelles and cowlings of various forms. The propeller was 4 feet in diameter in every case. The thick wing was of 5-foot chord and 15-foot span; the Clark Y wing, of 38-inch chord and 15-foot 10-inch span. The magnitude of these dimensions relative to each other and to the 20-foot-diameter air stream in which the tests were made are among the factors that determine the degree to which the tunnel tests reproduce flight conditions.

The validity of all the data reported in references 1 to 6 depends on the effects of certain departures from flight-operating conditions. The most obvious difference is the limited span of the test wing compared with the greater spans of actual wings used in flight. If the field of flow were appreciably altered beyond the tips of the test wing by the nacelle or the propeller, then the total effect that would be produced on a large airplane wing would be different from that measured on the test wing and the test data could not be applied directly to an airplane design. The "blocking" of such a large test wing in a 20-foot-diameter jet is another possible source of error in that a possible higher velocity near the edges of the stream, compared with the velocity in the center, is a condition not reproduced in flight. The jet boundary may also introduce undesirable effects.

British tests (reference 7), the only known experimental work on the subject, suggested that the influence of a nacelle without propeller extends about 6 or 7 diameters outboard of the nacelle center. Thus a wing of at least 20-foot span, or aspect ratio 4, would be required to measure the complete nacelle effect, and it might be supposed (in the absence of test results) that the propeller effect extends farther than the nacelle effect.

The influence of any such disturbing bodies as nacelles or propellers moving in free air obviously extends laterally an infinite distance. The disturbance is relatively great in the immediate vicinity of the disturbing element, but the magnitude of the flow change diminishes rather rapidly with increasing distance from its source and becomes asymptotic to a zero value. When a nacelle or a propeller or both are tested on a wing, they influence the flow over the whole of the wing, from tip to tip, regardless of the span. It is therefore improper to speak of a limit to, or a lateral extent of, the influence of nacelle or propeller and useless to

effects have been measured on the 15-foot-span wing. The blocking effect mentioned previously is considered to be a known quantity in the full-scale tunnel as a result of airplane tests and its numerical value is probably smaller than that for the same wing tested in the 20-foot tunnel. The jet-boundary corrections are also smaller, being, for a 15-foot-span wing, less than 30 percent of the values in the 20-foot tunnel because of the proportionately larger jet area. In order to define more closely the limits of the nacelle and propeller influences, pressure-distribution tests were made to give the required span-load curves.
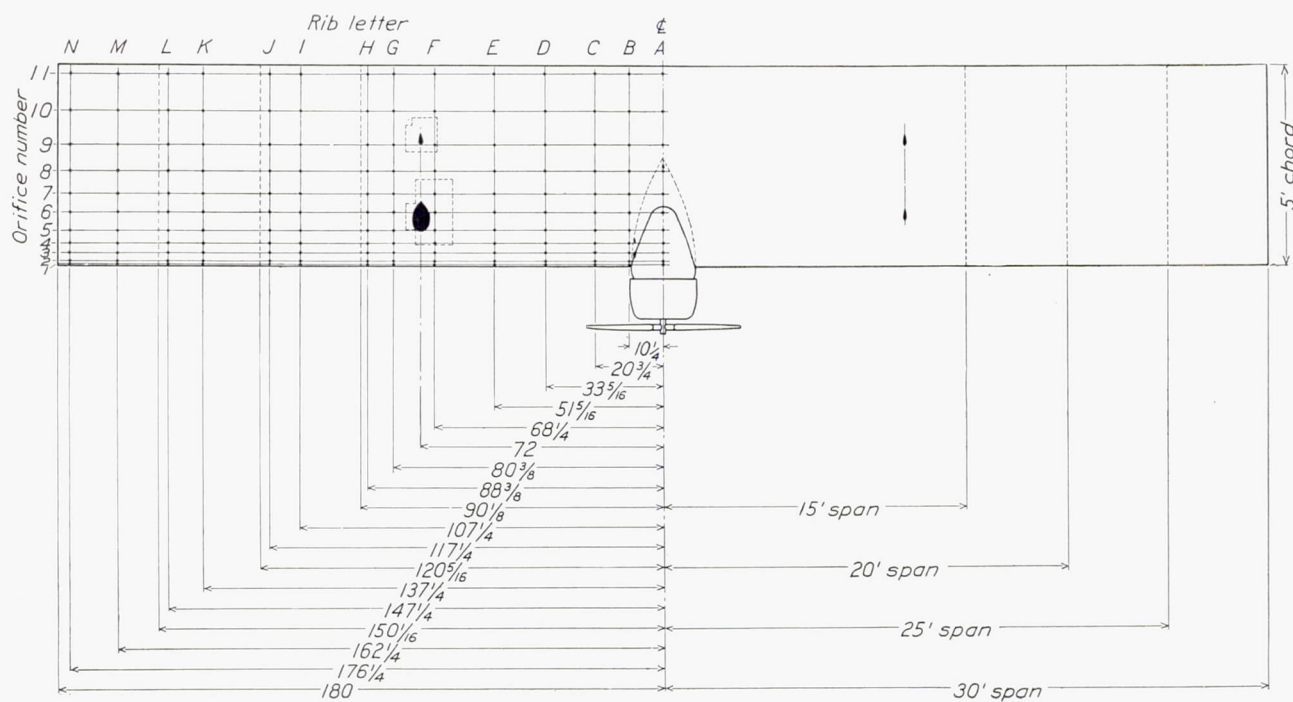

FIGURE 1.—Plan of test wing; lower surface showing pressure-orifice locations.

attempt to determine a wing span that includes within its tips the whole flow change. However, since the effect of nacelles and propellers becomes inappreciable for engineering usage at some distance laterally and becomes less than the limits of measurement at approximately the same point, it is convenient to consider the lateral extent of such effect to be the distance at which the local effect (for pressure-distribution tests) or the total effect (for force tests) becomes less than the limits of accuracy of the test for any increase of the span over which the effects are measured. Throughout the present paper the lateral extent is considered to have the limits just enumerated.

The present investigation was planned to evaluate the aforementioned effects in the full-scale wind tunnel. Force tests, repeated on wings of 5-foot chord and 15-, 20-, 25-, and 30-foot spans, were made to determine propulsive efficiencies, nacelle drag efficiency factors, and net efficiencies. Comparison of the values for the different spans shows to what extent the complete

APPARATUS AND METHODS

The full-scale wind tunnel, its balance, and the wing supports used in these tests are described in reference 8.

The apparatus will not be described in detail because a great deal of it is the same equipment that was used in the prior tests in the 20-foot tunnel. (See reference 1.) The wooden wing specially built for the tests to the ordinates specified in table I was of 30-foot span, 5-foot chord, and had a thickness equal to 20 percent of the chord. It was built to allow its being shortened symmetrically about its center to spans of 25, 20, and 15 feet. At each of 14 rib stations on the left half of the wing (fig. 1) 22 copper tubes terminated flush with the wing surfaces. These tubes passed inside the wing to flexible connections at the wing-support points. At the support points, the wing was provided either with large cut-outs through which the tubing passed during pressure-distribution tests or with small closely fitting cut-outs during force tests, the tubing being concealed inside the wing in the latter case. A number of flush

cover plates on the upper and lower surfaces of the center section were provided to allow attachment of the nacelle in various positions.

TABLE I.—WING ORDINATES

Station		Upper		Lower	
Percent chord	Inches	Percent chord	Inches	Percent chord	Inches
0	0	6.7	4.00	6.7	4.00
2.5	1.50	12.0	7.20	3.0	1.82
5	3.00	14.2	8.50	1.8	1.10
10	6.00	17.1	10.26	.6	.34
15	9.00	18.7	11.24	.2	.10
20	12.00	19.6	11.75	0	.02
30	18.00	20.0	12.00	0	0
40	24.00	18.9	11.34	0	0
50	30.00	16.9	10.14	0	0
60	36.00	14.1	8.48	0	0
70	42.00	11.0	6.58	0	0
80	48.00	7.5	4.52	0	0
90	54.00	3.8	2.30	0	0
100	60.00	0	0	0	0

The 4/9-scale model of a Wright J–5 radial air-cooled engine and N. A. C. A. cowled nacelle, the same as used in previous tests, is illustrated in figure 2. The

For pressure-distribution tests the orifices were connected to two multiple-tube manometers in the balance house by tubing attached to the support fairings. The recording manometers pictured in figure 4 are fully described in reference 9.

Force tests and pressure-distribution tests were made of the wing alone and of the wing with the nacelle in three positions. A 30-foot span wing was first used; by cutting and refinishing both tips, the span was reduced progressively to 25, 20, and 15 feet. Similar measurements were made in each case.

Figures 5 to 9 show the different spans, nacelle locations, and support conditions that make up the 32 combinations tested. Pressure-distribution tests were run, separately from the force tests, with the tubing that is attached to the strut fairings joined to the flexible ends of the tubing in the wing, and the bundle of connections faired, as nearly as could be, into a streamline shape as shown in figures 6 and 9.
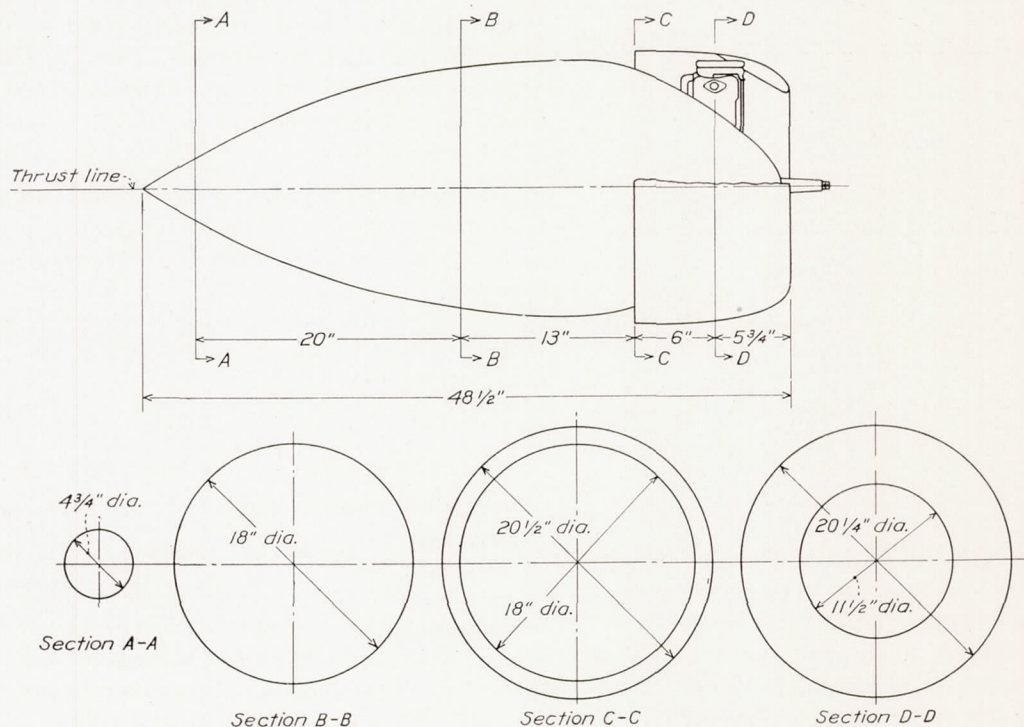
FIGURE 2.—The N. A. C. A. cowled nacelle and engine assembly.

nacelle contains a 25-horsepower 220-volt direct-current motor and an electric tachometer. A 4-foot aluminum-alloy model of the right-hand Navy No. 4412, 9-foot adjustable propeller, set 17° at 0.75 R, was normally used, but for a part of the pressure-distribution tests, to simulate flow over the half of the wing without pressure orifices, a geometrically similar left-hand propeller was fitted and pressure readings were taken on the same wing orifices as before. The three typical nacelle locations used in the present tests are shown in figure 3 and are designated by the numbering system of reference 1.

Force tests were made of the wing alone for each span at an air speed of approximately 60 miles per hour over an angle-of-attack range from —12° to 25° by 2° intervals, except that the intervals were closer near minimum drag and maximum lift. In addition, force tests and pressure-distribution measurements were made for the wing alone at angles of attack of —5°, 0°, 5°, 10°, and 15° at air speeds of approximately 30, 50, 80, and 100 miles per hour.

For each span and for each nacelle location, with propeller removed, force measurements at the same 5° intervals were made at various air speeds between 27

and 100 miles per hour. Pressure-distribution measurements were made at the same angles at air speeds of 30, 50, 80, and 100 miles per hour.

For each span and for each nacelle location, with right-hand propeller, propeller operating force tests were made at angles of attack of $-5°$, $0°$, $5°$, and $10°$ at 12 values of V/nD obtained by varying the air speed between 27 and 100 miles per hour and by throttling the motor at the highest air speed. Pressure-distribution tests were made at the same angles at four values of V/nD, between 0.23 and 0.76, obtained at approximately 30, 50, 80, and 100 miles per hour. Both types of test were repeated for the 15- and 30-foot spans with the left-hand propeller.

Tare force tests were made on the 30-foot-span wing by suspending it independently and measuring the air forces on the supports. The tare values obtained on the 30-foot-span wing were used for all spans.
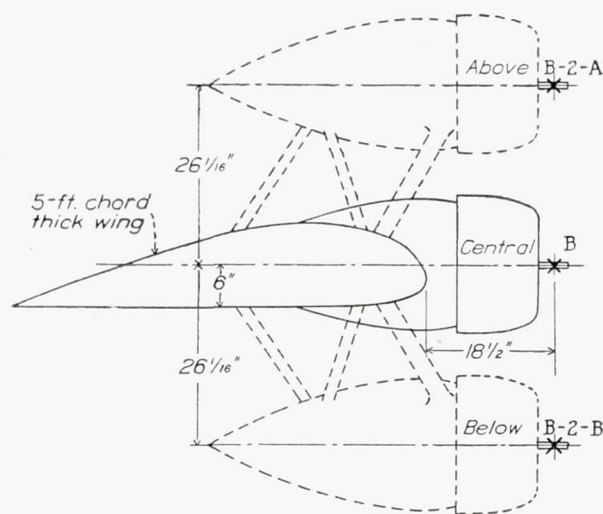

FIGURE 3.—Nacelle test locations.

In all force tests the lift, drag, angle of attack, and air speed were measured and, in the propeller-operating tests, the torque and propeller revolution speed in addition. Double or triple readings were taken for each test condition. In the pressure-distribution tests, single readings of angle of attack, air speed, and pressure at individual orifices were taken and, in tests with propeller operating, the propeller speed as well.

RESULTS

The conditions during these tests represent approximately one-fifth the full-scale Reynolds Number of a large, modern, high-speed transport airplane. The results for "high-speed flight," defined subsequently, were taken at about 88 miles per hour (Reynolds Number approximately 4,000,000) and those for "climbing flight" at about 57 miles per hour (Reynolds Number approximately 2,500,000). The degree of turbulence in the full-scale tunnel is discussed in references 10 and 11, which indicate that the effects of

turbulence are of secondary importance. The same references show that agreement may be expected between tests in the 20-foot tunnel and in the full-scale tunnel. For the purposes of this report the present results may be considered directly comparable, as regards scale and turbulence, with results from the 20-foot tunnel and may also be considered representative of flight conditions.

FORCE TESTS

The force-test data were corrected by the method described in reference 6 that allows comparison of different wing-nacelle combinations at the same angle of attack. This method involves computation of propulsive efficiencies, nacelle drag efficiency factors, and net efficiencies, all at the same angle of attack (for the same span), and correction for the jet-boundary drag and induced drag resulting from the differences in lift caused by the nacelle and propeller combinations. This procedure eliminates certain discrepancies that develop when the data are reduced in accordance with the method used in references 1 to 5. The corrections are explained in detail in reference 6, but the method and factors involved will be briefly enumerated in the following section.

Propulsive efficiency η is the ratio of the effective thrust power (total thrust power less loss caused by increased drag of parts in the slipstream) to the motor power.

$$\eta = \frac{\text{effective thrust} \times \text{velocity of advance}}{\text{motor power}}$$

$$= \frac{(T - \Delta D) V}{P}$$

$$= \frac{C_T}{C_P} \frac{V}{nD} + \frac{\Delta C_{D_i} + \Delta C_{D_j}}{C_P} \frac{S}{2D^2} \left(\frac{V}{nD}\right)^3$$

where all symbols have their usual meanings except as noted.

$$C_T = \frac{T - \Delta D}{\rho n^2 D^4}$$

where

T is thrust of propeller (shaft tension).

ΔD, change in drag of body (nacelle plus wing) due to action of propeller.

$T - \Delta D$, effective thrust, the quantity actually inferred from the measurements because of the difficulty in measuring T and ΔD separately; equal to the gross propeller-operating thrust of a wing-nacelle-propeller combination plus the drag of the same wing-nacelle combination, propeller off, at the same attitude and air speed.

ΔC_{D_i}, change in induced drag due to a change in lift. In the present case the lift change caused by the propeller is put in the form of the equivalent drag change by assuming the latter equal
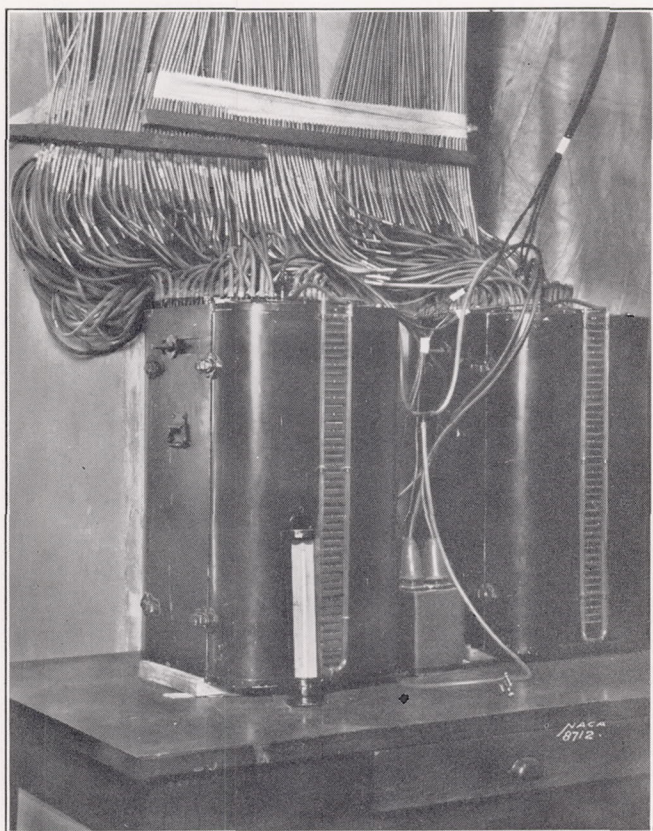
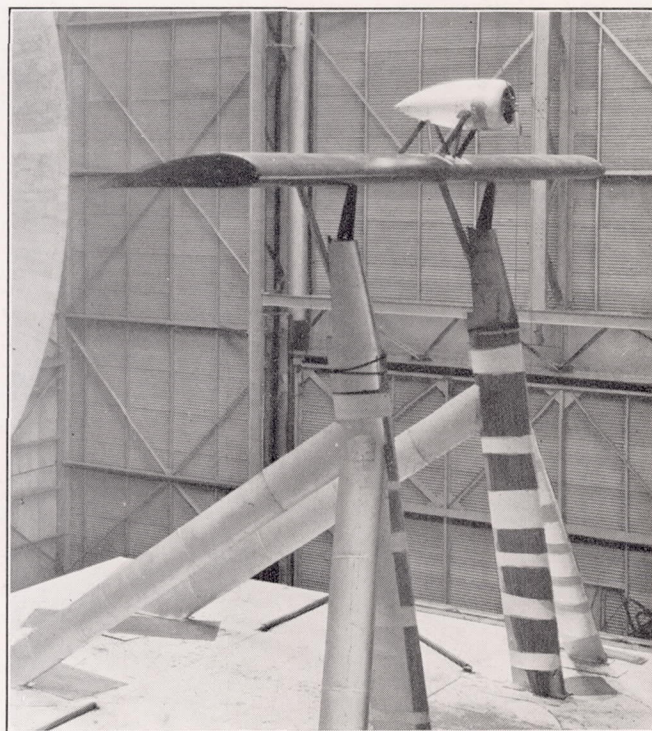FIGURE 4.—Multiple-tube recording manometers, model 4, connected for pressure-distribution tests.

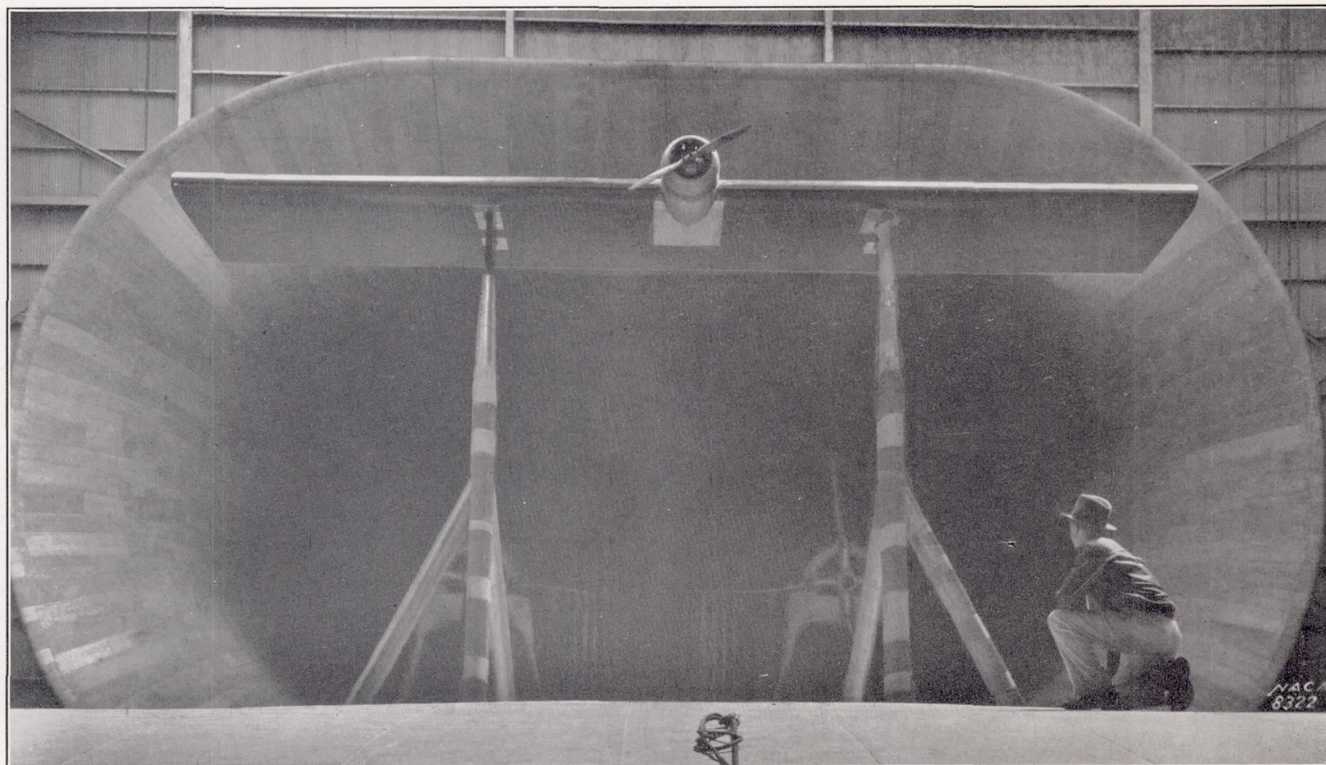FIGURE 5.—Force test; 5- by 30-foot wing, nacelle above.

FIGURE 6.—Pressure-distribution test; 5- by 30-foot wing, nacelle central.
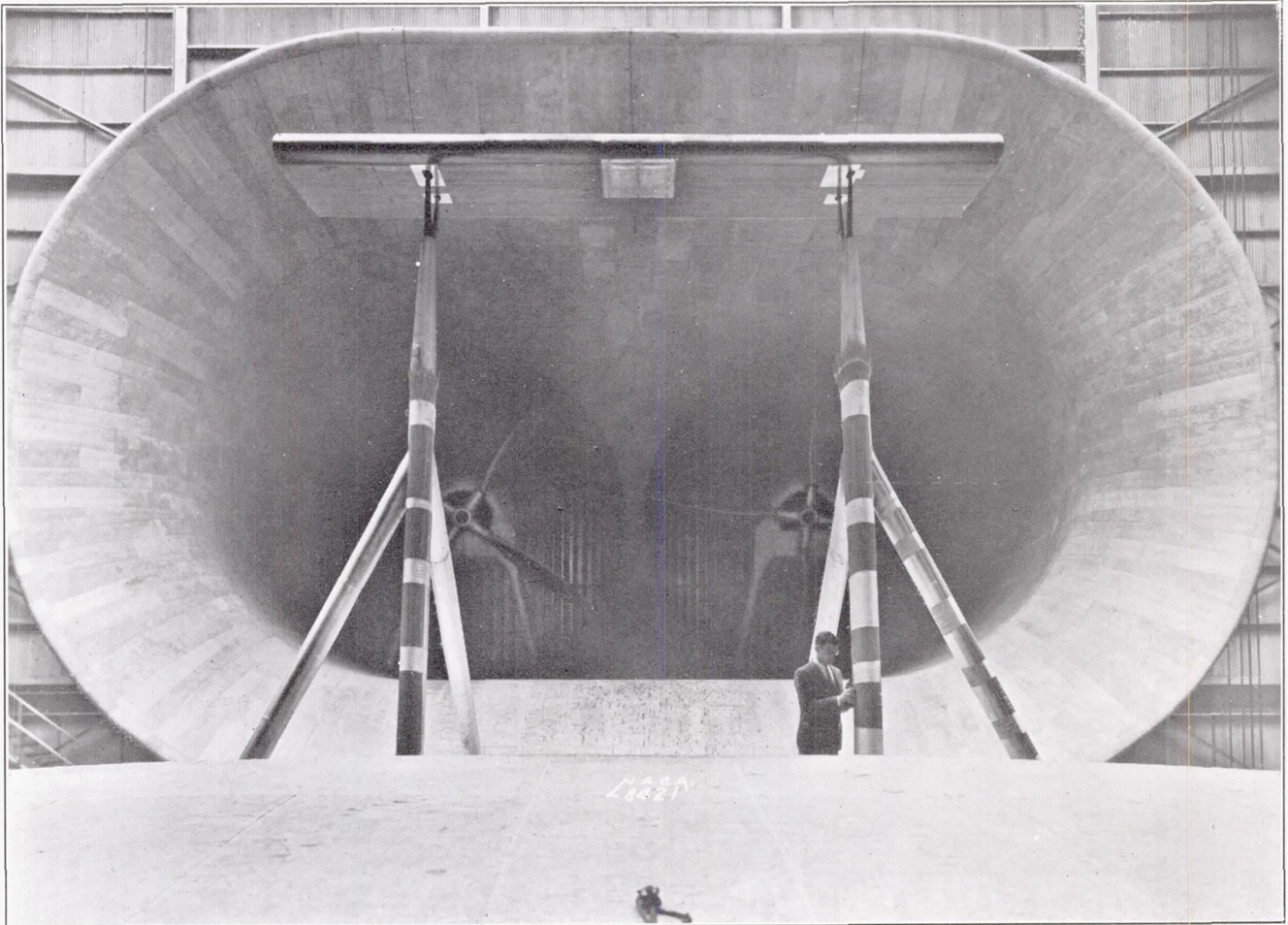
FIGURE 7.—Force test; 5- by 20-foot wing alone.
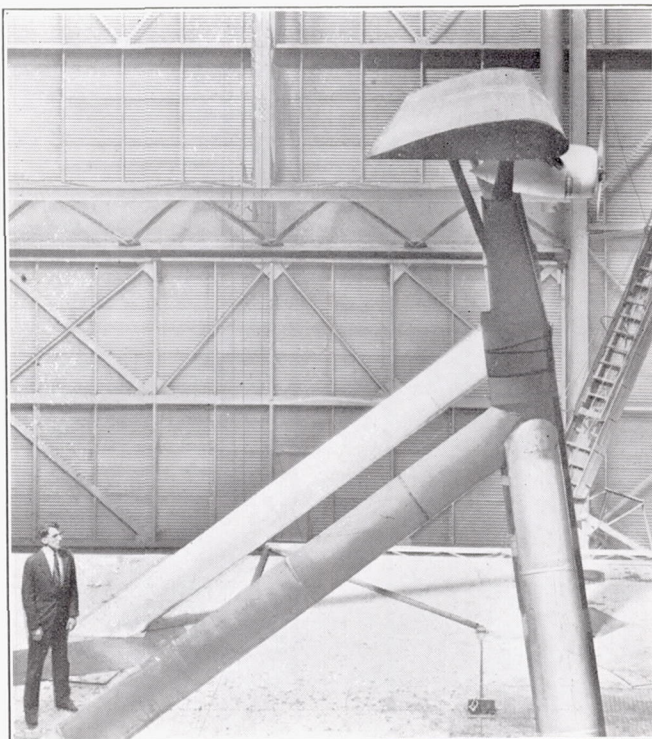

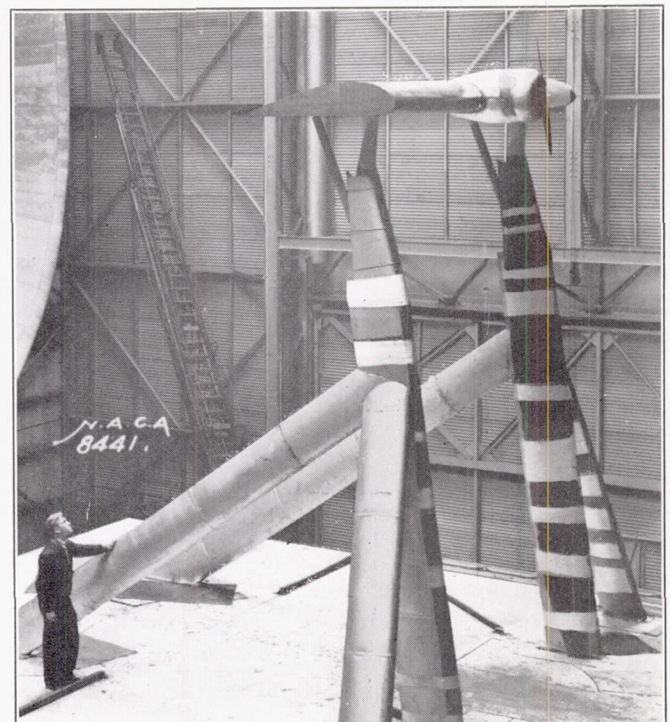FIGURE 8.—Force test; 5- by 25-foot wing, nacelle below.

FIGURE 9.—Pressure-distribution test; 5- by 15-foot wing, nacelle central.

to the change in induced drag experienced by an elliptically loaded wing of the same aspect ratio when its lift is changed from the actual measured lift, propeller removed, to the measured lift, propeller operating.

$$\Delta C_{D_i} = \frac{(C_{L_p}^2 - C_{L_c}^2)}{\pi \times A}$$

where

C_{L_p} is lift coefficient, propeller operating, of a wing-nacelle-propeller combination at a given angle of attack.

C_{L_c}, lift coefficient, propeller removed, of the same wing-nacelle combination at the same angle of attack.

A, aspect ratio.

ΔC_{D_j}, change in jet-boundary drag correction due to a change in lift; for the same reasons and based on the same lift change as ΔC_{D_i}.

$$\Delta C_{D_j} = \left(\delta \frac{S}{C}\right)(C_{L_p}^2 - C_{L_c}^2)$$

where

δ is the nondimensional jet-boundary correction factor.

C, cross-sectional area of the jet, 1,608 square feet.

Nacelle drag efficiency factor N. D. F. is the ratio of power absorbed by nacelle drag and interference to the motor power.

$$\text{N. D. F.} = \frac{(C_{D_c} - C_{D_w} + \Delta C_{D_i} + \Delta C_{D_j})}{C_P} \times \frac{S}{2D^2} \times \left(\frac{V}{nD}\right)^3$$

where

C_{D_w} is drag coefficient, wing alone, at a chosen angle of attack.

C_{D_c}, drag coefficient of wing-nacelle combination at the same angle of attack.

ΔC_{D_i}, change in induced drag due to a change in lift; in this case, the lift change caused by the nacelle.

$$\Delta C_{D_i} = \frac{(C_{L_w}^2 - C_{L_c}^2)}{\pi \times A}$$

C_{L_w}, lift coefficient of wing alone at the same angle of attack as C_{L_c} is taken.

ΔC_{D_j}, change in jet-boundary drag due to a change in lift; for the same reasons and based on the same lift change as ΔC_{D_i}.

$$\Delta C_{D_j} = \left(\delta \frac{S}{C}\right)(C_{L_w}^2 - C_{L_c}^2)$$

Net efficiency η_0 is the percentage of the motor power available for uses other than for overcoming the losses,

direct and indirect; of the nacelle-propeller combination; that is, the fraction of the engine brake horsepower available for overcoming the drag of the complete airplane without nacelles, nacelle supports, if any, and propellers.

$$\eta_0 = \eta - \text{N. D. F.}$$

The results are compared for two flight conditions: $C_L = 0.2$, $V/nD = 0.65$; and $C_L = 0.6$, $V/nD = 0.42$, values which represent high-speed (not necessarily full-speed) and climbing conditions, respectively, for airplanes utilizing the pitch setting used in these tests $(17°)$. The three types of tests—wing alone, wing and nacelle with propeller removed, and wing-nacelle combination with propeller operating—were all compared, for any one span, at the same two angles of attack at which the wing alone showed the chosen lift coefficients; differences in lift were taken into account as detailed in reference 6 and as described briefly in the preceding paragraphs. All results were corrected for blocking and for the air-stream angle known to exist in the tunnel. Both these corrections were determined by airplane tests and by Clark Y airfoil tests reported in reference 10 and by air-stream surveys made in the jet. All results are finally corrected for jet-boundary effects. The values of the factor δ used for these corrections are: -0.203 for 15-foot span, -0.206 for 20-foot span, -0.208 for 25-foot span, and -0.210 for 30-foot span.

Results of the force tests are summarized in figure 10, which shows the variation of propulsive efficiency, nacelle drag efficiency factor, and net efficiency with span. The plotted points are not observed values but are computed from values taken from faired curves. They are included only to show the degree of dispersion from the faired curve. Since the present comparisons are made at different values of C_L than those chosen in reference 1, the results are also compared for the conditions ($C_L = 0.409$, $V/nD = 0.65$; $C_L = 0.652$, $V/nD = 0.42$) used in that reference and the numerical values are given in table II.

TABLE II.—COMPARISON OF 15-FOOT-SPAN RESULTS

Tunnel	Nacelle above			Nacelle central			Nacelle below		
	N. D. F.	η	η_0	N. D. F.	η	η_0	N. D. F.	η	η_0
High speed; $\alpha = 0°$; $C_L = 0.409$; $V/nD = 0.65$									
20-foot [1]	0.155	0.802	0.647	0.042	0.776	0.734	0.086	0.763	0.677
Full-scale [2]	.137	.784	.647	.051	.813	.762	.097	.794	.697
Climbing; $\alpha = 5°$; $C_L = 0.652$; $V/nD = 0.42$									
20-foot [1]	0.035	0.663	0.628	0.017	0.683	0.666	0.028	0.644	0.616
Full-scale [2]	.034	.677	.643	.020	.734	.714	.005	.659	.654

[1] Data from reference 1, corrected by method of reference 6.
[2] Data from present tests, corrected by method of reference 6.

Complete polars of the wing and wing-nacelle combinations (fig. 11) for the four spans show the variation of nacelle drag with lift coefficient. It is apparent, however, that if the nacelle drags are identical when nacelles are mounted on two wings of unequal span and area, other conditions being the same, the nacelle drag coefficients will not be the same in both cases because of the different wing areas on which the coefficients are
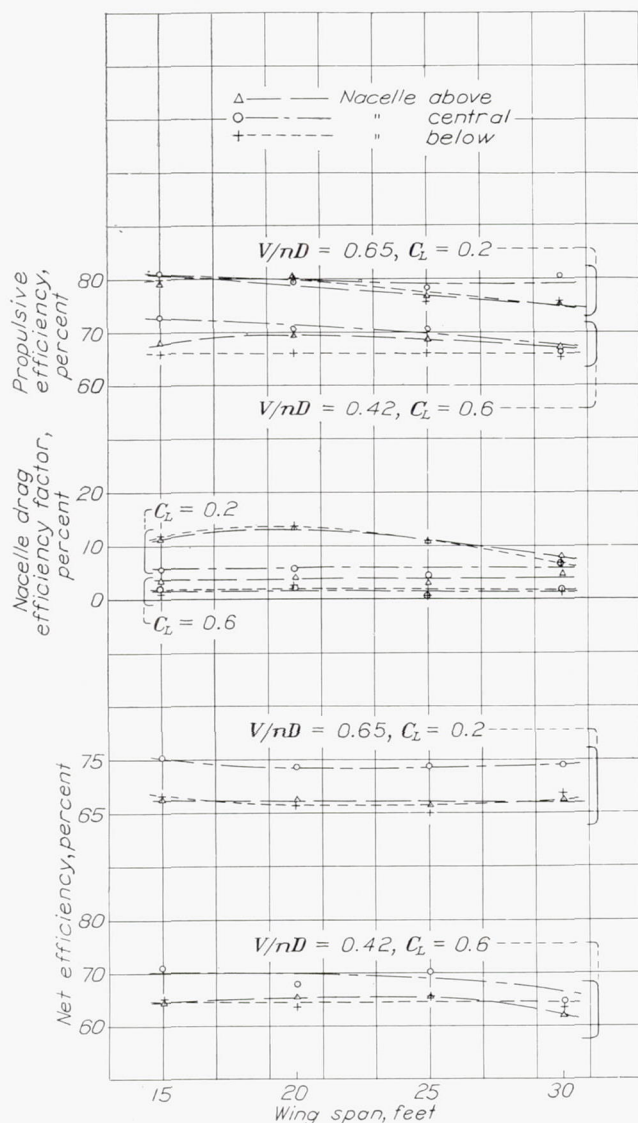

FIGURE 10.—Variation with span of nacelle-propeller efficiency factors.

based; that is, on the 30-foot-span wing a nacelle drag of 4.6 pounds at 100 miles per hour gives a nacelle drag coefficient ΔC_D of 0.0012; whereas, if the nacelle has the same drag when mounted on the 15-foot-span wing, the nacelle drag coefficient ΔC_D is equal to 0.0024 based on the reduced wing area. In order that any variation with span, as well as variation with lift coefficient, may be shown on a plot of nacelle drag coefficients, each coefficient is multiplied by a factor K equal to the ratio of the wing areas and the result is termed the "effective

nacelle drag coefficient." This coefficient is then a constant independent of span or area if the actual nacelle drag is constant for different spans. The factors and the resulting effective nacelle drag coefficients are shown in figure 12. In figure 13 the variation of effective nacelle drag coefficient with span is shown for the three nacelle positions at the high-speed condition.

In figure 14 are plotted some results obtained incidentally during the main research. They show the variation with span of effective profile drag coefficient at $C_L=0.2$, maximum lift coefficient, and angle of attack for maximum lift, all corrected to free-air conditions.

PRESSURE-DISTRIBUTION TESTS

The basis for comparison of the pressure-distribution tests is the same as for the force tests, i. e., high-speed and climbing conditions, with the same criterions as in the force tests. The normal-force coefficient C_N for each rib was first plotted against angle of attack α and, for propeller-operating tests, at a constant V/nD. At the angle of attack at which the force tests showed that the chosen C_L would be realized, the value of C_N for each rib was read. For propeller-operating tests these points were cross-plotted against V/nD and values at the chosen V/nD were used. These values of rib C_N were then plotted at appropriate rib positions to give the span loading for the two flight conditions considered.

Results of the pressure-distribution tests are collected in figures 15, 16, and 17. These figures show the span-load curves for high-speed and climbing flight for the wing alone and for the nacelle above, central, and below. The charts show the loading as seen from upstream, looking at the leading edge, with the propeller turning in the direction indicated. The plotted points are not observed values but are obtained by cross-fairing and are included as the best guide in judging the limits to which the curves should be read. For the following reasons the curves do not show directly the resultant free-air load distribution of the complete span. Measurements were taken on only one half of the wing and a left-hand propeller was used to simulate the slipstream effect on the other half of the wing. A blocking effect in the tunnel (reference 12) results in slightly different local velocities at each rib; but, for simplicity, the rib coefficients are computed on the basis of average velocity. No correction for the jet boundary was made to the span loading, but this effect is known to be small. The previously mentioned conditions, however, do not make the results any less valid for the present comparison; in fact, the use of right- and left-hand propellers eliminates the effect of any asymmetry of air flow and wing profile and permits an easier and more accurate determination of the slipstream effect.

PRECISION

The precision of the force tests was about the same as for the earlier tests in the 20-foot tunnel. The angle of attack of the wing was set within 0.1°. Tachometer readings were accurate to within one-half of 1 percent. Lift readings were taken to the nearest pound and drag

results should be accurate to within ±2 percent for the efficiencies and ±20 percent at low lift coefficients for the nacelle drag coefficients.

The pressure-distribution results are less precise than the force results. Only single observations were taken for a given set of conditions but cross-fairing tended to
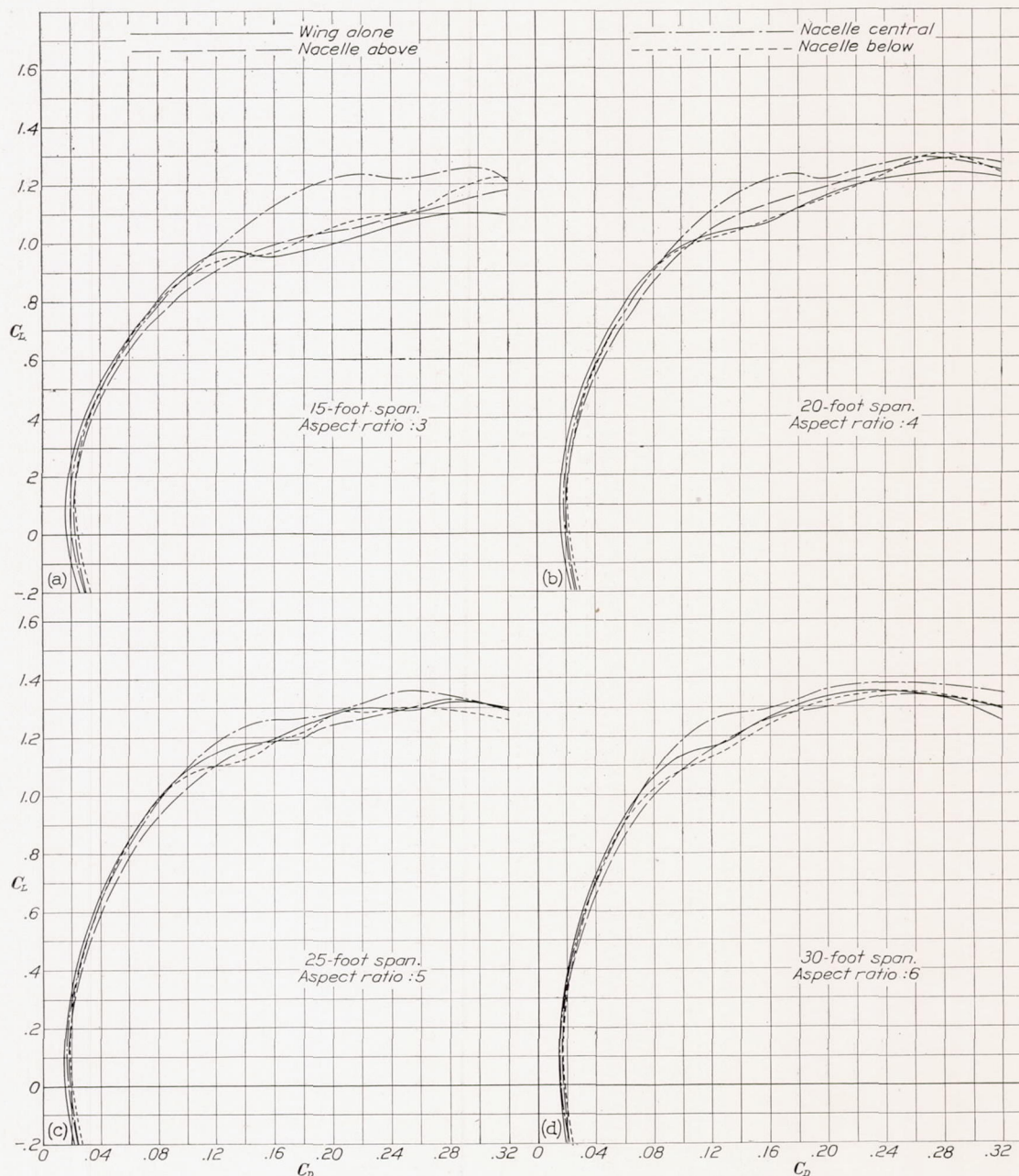

FIGURE 11. (a, b, c, d).—Comparison of lift and drag characteristics of wing alone and N. A. C. A. cowled nacelle combination, propeller removed, in three positions, corrected for tunnel effects; Reynolds Number, 2,800,000; full-scale tunnel.

readings to the nearest 0.1 pound. The magnitude of the tare forces aided in securing high accuracy; tare drag was approximately 7 percent of $C_{D_{min}}$ for the 15-foot span and approximately 4 percent for the 30-foot span. The over-all precision is, of course, less on the larger spans on account of obtaining small differences by deducting forces of correspondingly larger magnitudes. On the 15-foot span, at least, the final

diminish the effect of individual erratic readings. The scatter of points on plots of rib C_N against α shows the dispersion to be more nearly a given absolute value than a given percentage so that the accuracy will be less at the lower lift coefficients. Below the stall, however, the dispersion of observed points might be placed at ±5 percent and the accuracy of the final span-load curves at ±3 percent.

DISCUSSION

FORCE TESTS

An examination of figure 10 indicates the extent to which the nacelle-propeller efficiency factors may vary with the span of the test wing. Propulsive efficiencies, factors show the same tendency except that the indicated variation is greater in some cases. The nacelle drag efficiency factor is useful mainly for comparison with results previously reported; a more useful and more accurately determined quantity and its variation
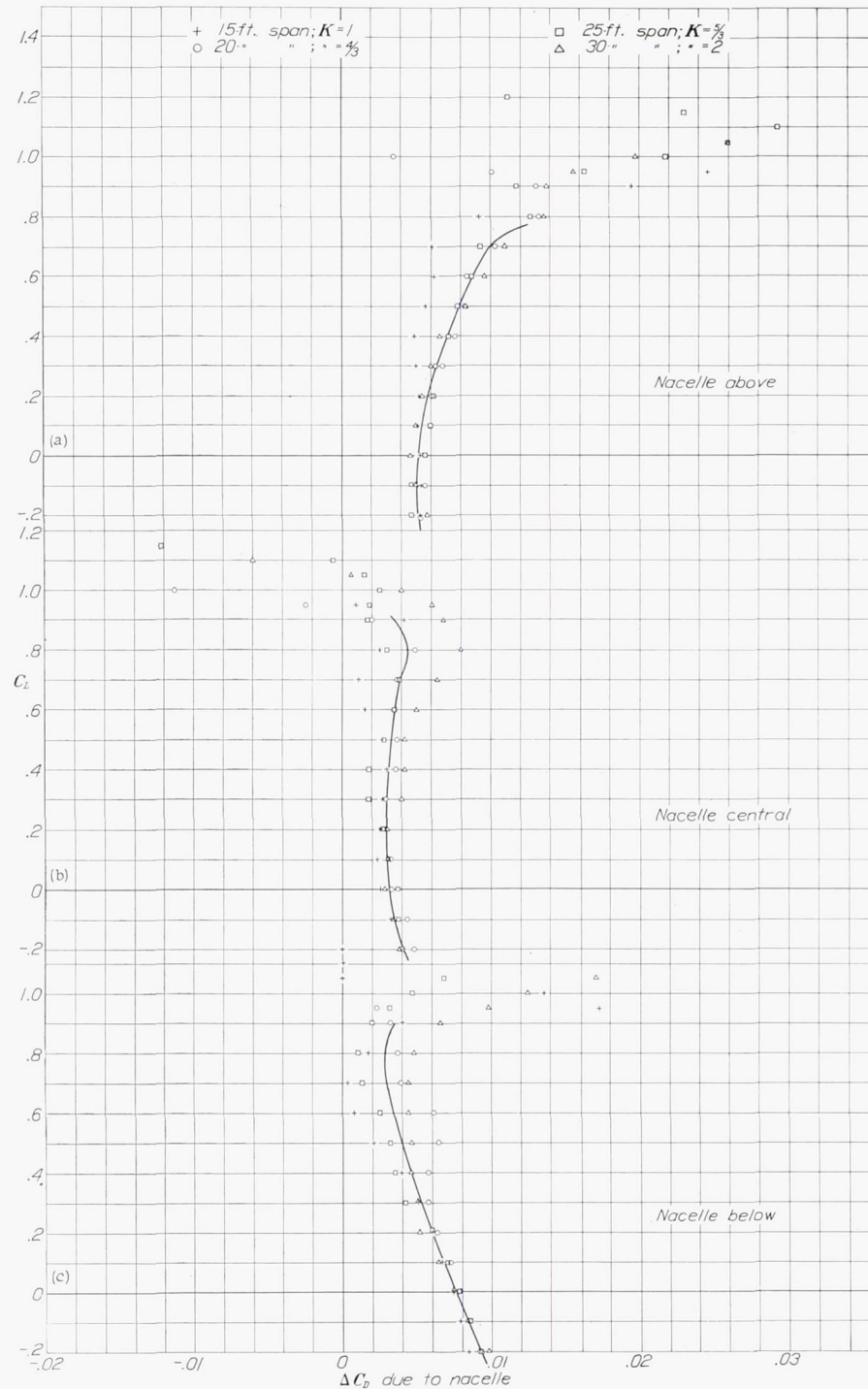

FIGURE 12 (a, b, c).—Effective nacelle drag coefficients for four spans. Based on wing area of 75 square feet; engine diameter, 20 inches. $\Delta C_D = K(C_{D_c} - C_{D_u})$.

both in high-speed and climbing conditions, generally tend to increase slightly as the wing is shortened from 30 to 15 feet. The best combination, nacelle central, shows small variation in propulsive efficiency, especially at the high-speed condition. The nacelle drag efficiency with span will presently be discussed. A comparison of the propulsive-efficiency curves and the curves of the nacelle drag efficiency factor demonstrates that the propeller, in spite of its larger diameter, is no more affected by span than is the nacelle. Because the

propulsive-efficiency curves and N. D. F. curves have similar tendencies, the net-efficiency curves show even less variation with span than the curves from which they are derived. The maximum over-all variation of any of the net-efficiency curves is little over 3 percent. These curves generally show their greatest departure from constant values for the 30-foot span for which the experimental errors are known to be largest.
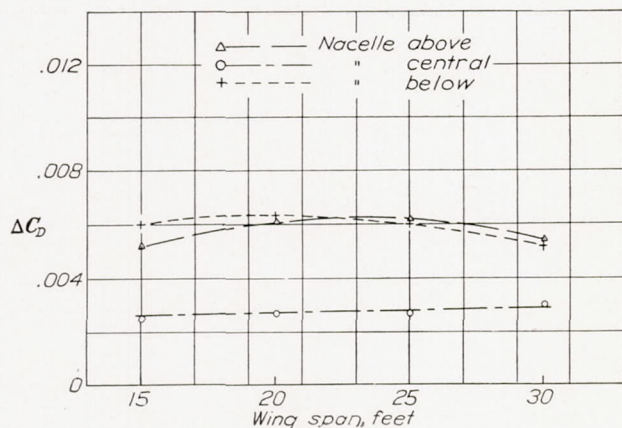

FIGURE 13.—Variation with span of effective nacelle drag coefficients for $C_L=0.2$.

It has been determined (reference 13) that the most accurate way to apply nacelle-propeller data to airplanes, the design speed of which is considerably in excess of the wind-tunnel speeds at which the data were taken, as is now usually the case, is to use an experimentally determined propulsive efficiency and the effective nacelle drag coefficient (which includes interference) scaled to the proper engine size and wing area, instead of using a net efficiency value. At the higher flying speeds the nacelle drag assumes a greater importance than formerly and accurate data on this portion of the airplane loss are accordingly more valuable. For this reason the nacelle drag, in the form of an effective nacelle drag coefficient, is obtained from the original data with as little loss in accuracy as possible by taking the difference in effective profile drag coefficients, nacelle off and nacelle on, at the same lift coefficients. These results (fig. 12) are readily usable for design purposes; it is recommended that the faired-curve values be used in each case. Because of their simple and more accurate derivation and because the results are represented for the whole useful-lift range instead of for the two conditions ($C_L=0.2$ and $C_L=0.6$) previously used, these results provide a good basis for judging the effect of span.

All the results cited thus far, especially the curves of effective nacelle drag coefficient, indicate no systematic variation of nacelle and interference drag with span and imply that all effects, within the precision of the measurements, are therefore included by the 15-foot-span wing. Figure 13, derived from figure 12, is typical and illustrates the condition for a high-speed lift-coefficient value. Similar figures, constructed for

larger values of lift coefficient, show a greater dispersion of points but cannot definitely be interpreted to show consistent variations of nacelle and interference drag with span.

The comparison in table II of 20-foot-tunnel data with the corresponding data from the full-scale tunnel demonstrates that both series of tests are substantially in agreement. As explained in reference 6, the pro-
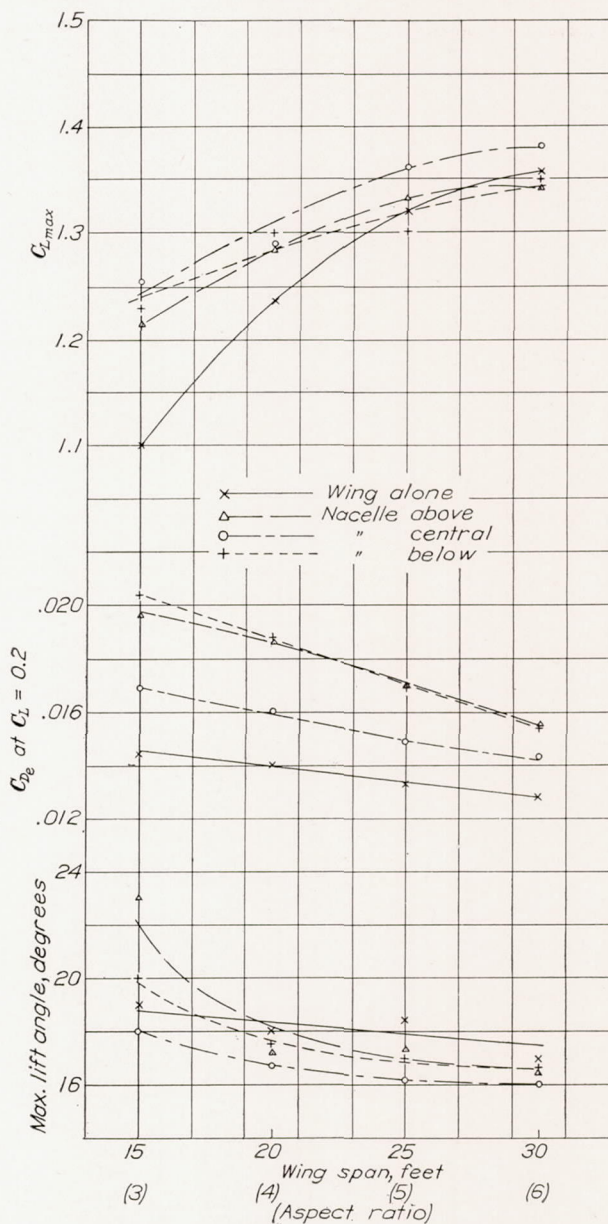

FIGURE 14.—Variation with span of wing-nacelle characteristics. Corrected for tunnel effects; Reynolds Number 2,800,000; full-scale tunnel.

pulsive efficiencies and nacelle drag efficiency factors given in reference 1 will change when corrected for the induced-drag effects but, because the power coefficients and lift-curve slopes remain nearly constant, the net efficiencies will not change perceptibly.

The values of all quantities measured in the full-scale wind tunnel are generally higher than those from the 20-foot tunnel but, compared with the precision of the
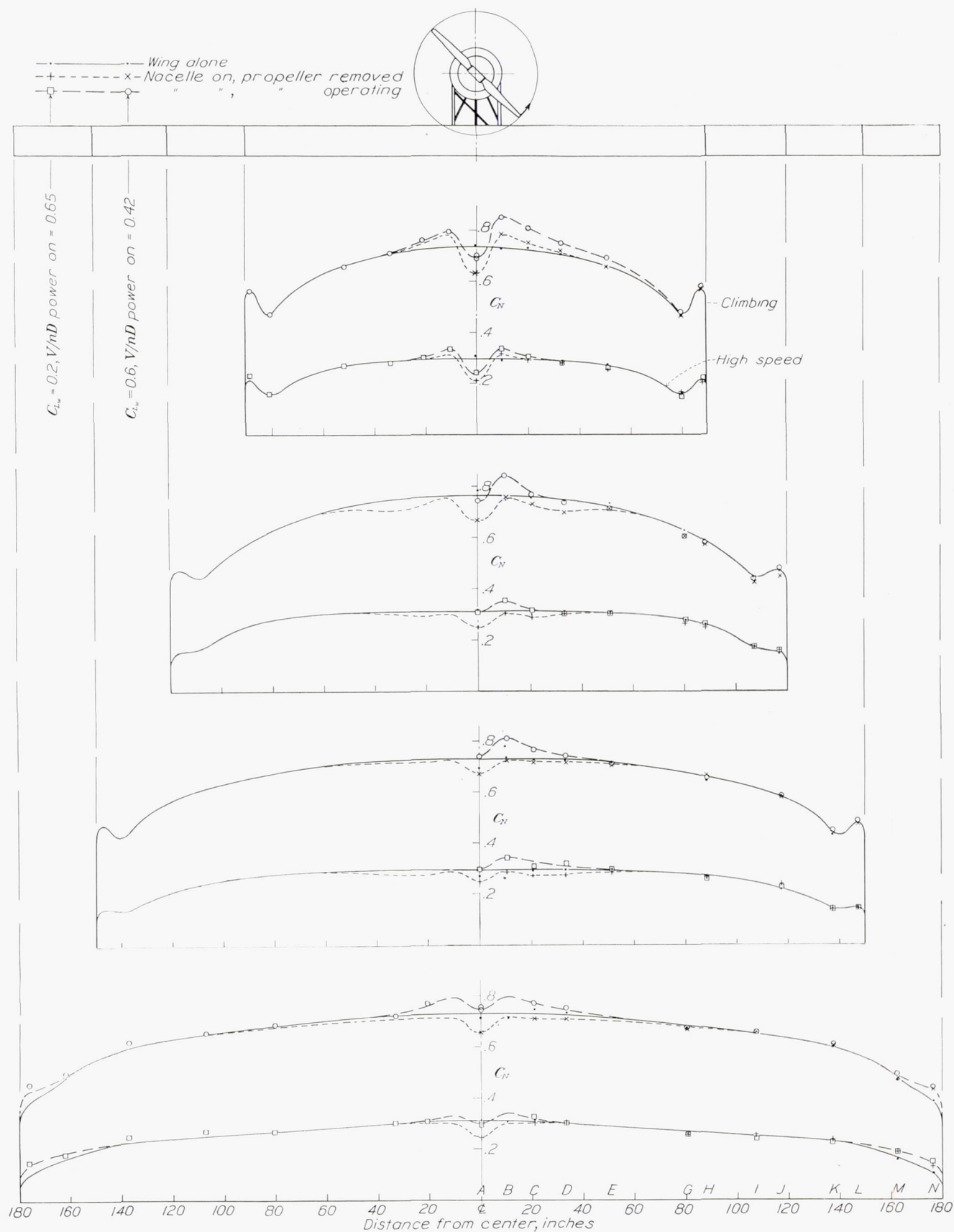
FIGURE 15.—Span-load curves. Wing alone and nacelle *above*; propeller removed and propeller operating; various spans.
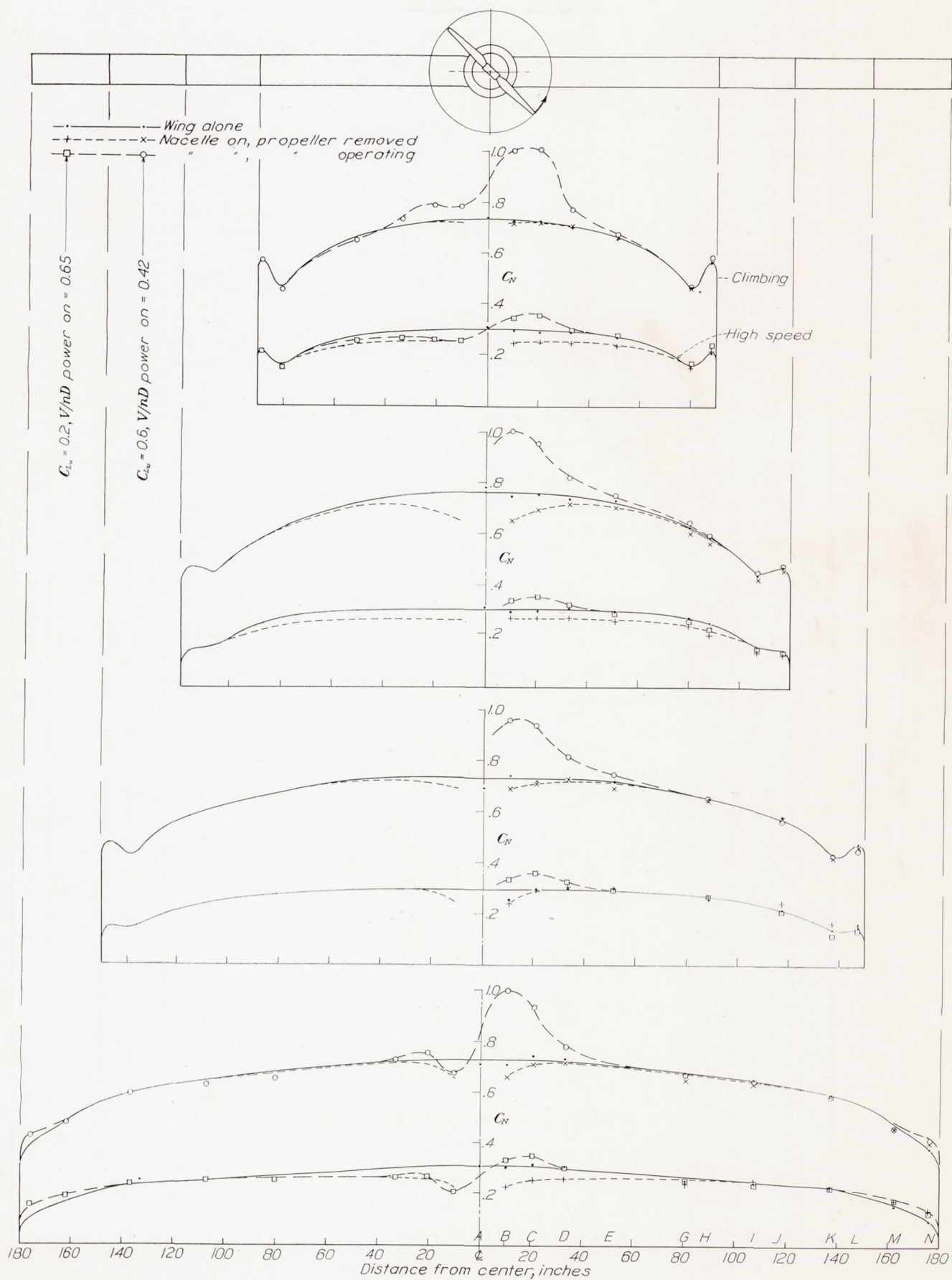
FIGURE 16.—Span-load curves. Wing alone and nacelle *central;* propeller removed and propeller operating; various spans.

FIGURE 17.—Span-load curves. Wing alone and nacelle *below;* propeller removed and propeller operating; various spans.

tests, the difference is not great. Propulsive efficiencies for the three nacelle locations average 0.017 higher for high-speed and 0.026 higher for climbing; nacelle drag efficiency factors average 0.001 higher for high-speed and 0.008 higher for climbing; and net efficiencies average 0.016 and 0.034 higher, respectively.

The incidental results plotted in figure 14 show the usual trend for wings of medium aspect ratio. The wings with nacelles show decreasing maximum lift coefficients as the aspect ratio is decreased from 6 to 3, but the decrease is only about half that for the wing alone. The minimum drag coefficient of the wing alone increases with decreasing aspect ratio because a tip loss, which must be nearly constant in absolute value for the spans tested, accounts for a larger portion of the coefficient as the area is reduced. In the same way the nacelle, with its drag a constant independent of span, raises the coefficient most for the shortest span because of the smaller area on which the coefficient is based. If allowance is made for this fact, the variation of minimum drag coefficient is about the same for the wing-nacelle combinations as for the wing alone. The various combinations show an increase of angle for maximum lift, with decrease of aspect ratio, similar to the wing alone except that the increase is more rapid for the lower aspect ratios.

PRESSURE-DISTRIBUTION TESTS

If only the more marked effects that would be important in engineering practice are considered, the pressure-distribution curves of span load (figs. 15, 16, and 17) also show that the nacelle and propeller effects do not extend appreciably beyond the limits of a 15-foot-span wing, approximately four and one-half nacelle diameters or two propeller diameters outboard of the center. Figure 15, nacelle above the wing, shows that the effects of the nacelle extend in no case beyond 80 or 100 inches (four or five nacelle diameters) from the center. Figure 16, nacelle central, shows that although the loading at the center is changed more radically than for nacelle above or below, the effects do not extend beyond 100 inches. Figure 17, nacelle below the wing, shows that the effects of the nacelle extend about 100 inches as a maximum. Contrary to the previously expressed supposition, most of the curves show that the lateral extent of the propeller effect is no greater than that of the nacelle without propeller.

Consideration of the degree to which all the nacelle locations tested in the present research indicate like values of the lateral extent of their influence and consideration of the results of reference 7, which indicate that the magnitude, but not the lateral extent,

of the interference increases for high-drag nacelles (comparable to uncowled engines) and very poor locations (touching the upper or lower surface of the wing), lead one to believe that the present conclusions are applicable to usual wing-nacelle-propeller combinations. One of the variables not tested was wing thickness, but this variable is shown by other results (reference 3) to be of secondary importance. The case of the pusher propeller probably represents the greatest departure, but this case probably affects wing-nacelle characteristics less because the inflow, in which a part of the wing lies, is more regular and of smaller intensity than the slipstream of a tractor propeller.

The present tests indicate that the optimum span on which to test the 4/9-scale nacelle and propeller in a large wind tunnel is about 20 feet (semispan equal to six nacelle diameters or two and one-half propeller diameters, approximately). For smaller spans the pressure-distribution results show appreciable effects, in some cases to the point at which the tip effects begin, a condition which it seems desirable to eliminate. For larger spans the precision of the force tests decreases. The 15-foot span wing, however, is sufficiently large to measure all effects within practical limits of accuracy.

CONCLUSIONS

1. Force and pressure-distribution tests concur in indicating that for engineering purposes the influence of a nacelle may be considered to extend laterally along a wing no farther than about five nacelle diameters from its center.

2. Similar tests indicate that a propeller operating with a usual wing-nacelle combination may be considered to influence the wing no farther laterally than does the nacelle alone, that is, about two propeller diameters from its center.

3. All important effects of a 4/9-scale nacelle-propeller combination may be measured within practical limits of accuracy on a 15-foot-span wing in the jet of the 20-foot tunnel.

4. The present test results show substantial agreement, for the same operating conditions, with results previously obtained in the 20-foot tunnel.

5. The foregoing conclusions probably apply approximately to all usual wing-nacelle-propeller combinations.

REFERENCES

1. Wood, Donald H.: Tests of Nacelle-Propeller Combinations in Various Positions with Reference to Wings. Part I—Thick Wing—N. A. C. A. Cowled Nacelle—Tractor Propeller. T. R. No. 415, N. A. C. A., 1932.

2. Wood, Donald H.: Tests of Nacelle-Propeller Combinations in Various Positions with Reference to Wings. II—Thick Wing—Various Radial-Engine Cowlings—Tractor Propeller. T. R. No. 436, N. A. C. A., 1932.

3. Wood, Donald H.: Tests of Nacelle-Propeller Combinations in Various Positions with Reference to Wings. III—Clark Y Wing—Various Radial-Engine Cowlings—Tractor Propeller. T. R. No. 462, N. A. C. A., 1933.

4. McHugh, James G.: Tests of Nacelle-Propeller Combinations in Various Positions with Reference to Wings. IV—Thick Wing—Various Radial-Engine Cowlings—Tandem Propellers. T. R. No. 505, N. A. C. A., 1934.

5. Valentine, E. Floyd: Tests of Nacelle-Propeller Combinations in Various Positions with Reference to Wings. V—Clark Y Biplane Cellule—N. A. C. A. Cowled Nacelle—Tractor Propeller. T. R. No. 506, N. A. C. A., 1934.

6. Wood, Donald H., and Bioletti, Carlton: Tests of Nacelle-Propeller Combinations in Various Positions with Reference to Wings. VI—Wings and Nacelles with Pusher Propeller. T. R. No. 507, N. A. C. A., 1934.

7. Ower, E., and Hutton, C. T.: On the Interference of a Streamline Nacelle on a Monoplane Wing. R. & M. No. 1395, British A. R. C., 1931.

8. DeFrance, Smith J.: The N. A. C. A. Full-Scale Wind Tunnel. T. R. No. 459, N. A. C. A., 1933.

9. Parsons, John F.: Full-Scale Force and Pressure-Distribution Tests on a Tapered U. S. A. 45 Airfoil. T. N. No. 521, N. A. C. A., 1935.

10. Silverstein, Abe: Scale Effect on Clark Y Airfoil Characteristics from N. A. C. A. Full-Scale Wind-Tunnel Tests. T. R. No. 502, N. A. C. A., 1934.

11. Platt, Robert C.: Turbulence Factors of N. A. C. A. Wind Tunnels as Determined by Sphere Tests. T. R. No. 558, N. A. C. A., 1936.

12. Theodorsen, Theodore, and Silverstein, Abe: Experimental Verification of the Theory of Wind-Tunnel Boundary Interference. T. R. No. 478, N. A. C. A., 1934.

13. Wood, Donald H.: Engine Nacelles and Propellers and Airplane Performance. S. A. E. Jour., April 1936, pp. 148–160.
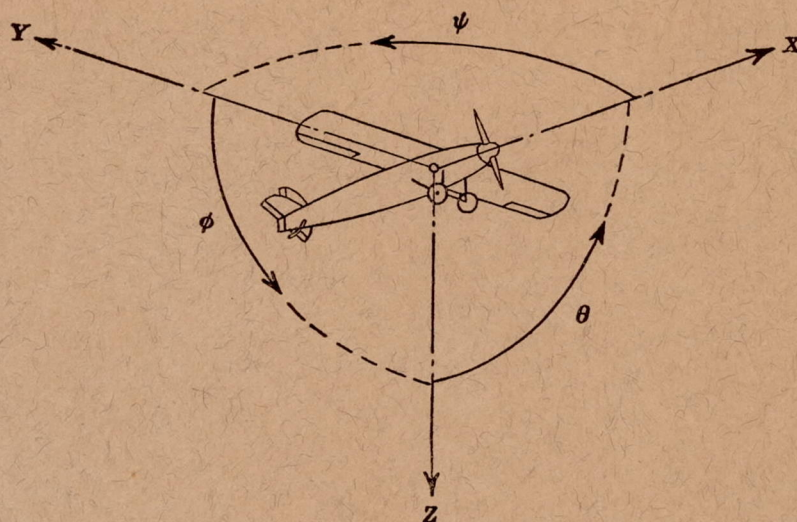
Positive directions of axes and angles (forces and moments) are shown by arrows

Axis		Force (parallel to axis) symbol	Moment about axis			Angle		Velocities	
Designation	Symbol		Designation	Symbol	Positive direction	Designation	Symbol	Linear (component along axis)	Angular
Longitudinal	X	X	Rolling	L	$Y \longrightarrow Z$	Roll	ϕ	u	p
Lateral	Y	Y	Pitching	M	$Z \longrightarrow X$	Pitch	θ	v	q
Normal	Z	Z	Yawing	N	$X \longrightarrow Y$	Yaw	ψ	w	r

Absolute coefficients of moment

$$C_l = \frac{L}{qbS} \qquad C_m = \frac{M}{qcS} \qquad C_n = \frac{N}{qbS}$$
$$\text{(rolling)} \qquad\quad \text{(pitching)} \qquad\quad \text{(yawing)}$$

Angle of set of control surface (relative to neutral position), δ. (Indicate surface by proper subscript.)

4. PROPELLER SYMBOLS

D,   Diameter
p,   Geometric pitch
p/D,   Pitch ratio
V',   Inflow velocity
V_s,   Slipstream velocity

T,   Thrust, absolute coefficient $C_T = \dfrac{T}{\rho n^2 D^4}$

Q,   Torque, absolute coefficient $C_Q = \dfrac{Q}{\rho n^2 D^5}$

P,   Power, absolute coefficient $C_P = \dfrac{P}{\rho n^3 D^5}$

C_s,   Speed-power coefficient $= \sqrt[5]{\dfrac{\rho V^5}{P n^2}}$

η,   Efficiency
n,   Revolutions per second, r.p.s.

Φ,   Effective helix angle $= \tan^{-1}\left(\dfrac{V}{2\pi rn}\right)$

5. NUMERICAL RELATIONS

1 hp. = 76.04 kg-m/s = 550 ft-lb./sec.
1 metric horsepower = 1.0132 hp.
1 m.p.h. = 0.4470 m.p.s.
1 m.p.s. = 2.2369 m.p.h.

1 lb. = 0.4536 kg.
1 kg = 2.2046 lb.
1 mi. = 1,609.35 m = 5,280 ft.
1 m = 3.2808 ft.